

Some topics in hadron production from heavy ion collisions

Che-Ming Ko
Texas A&M University

- Introduction: kaon production and nuclear EOS
- Charged pion ratio: nuclear symmetry energy
- Pion production at high energy: in-medium effects
- Deep subthreshold Ξ production: heavy baryonic resonances
- Charmed baryon production at RHIC and LHC: diquarks
- Lambda polarization: vorticity and shear
- Exotic hadrons: hadronic molecules vs compact multiquark states
- Summary

Supported by U.S. Department of Energy

First experiment on strangeness production in HIC

Production of K^+ Mesons in 2.1-GeV/Nucleon Nuclear Collisions

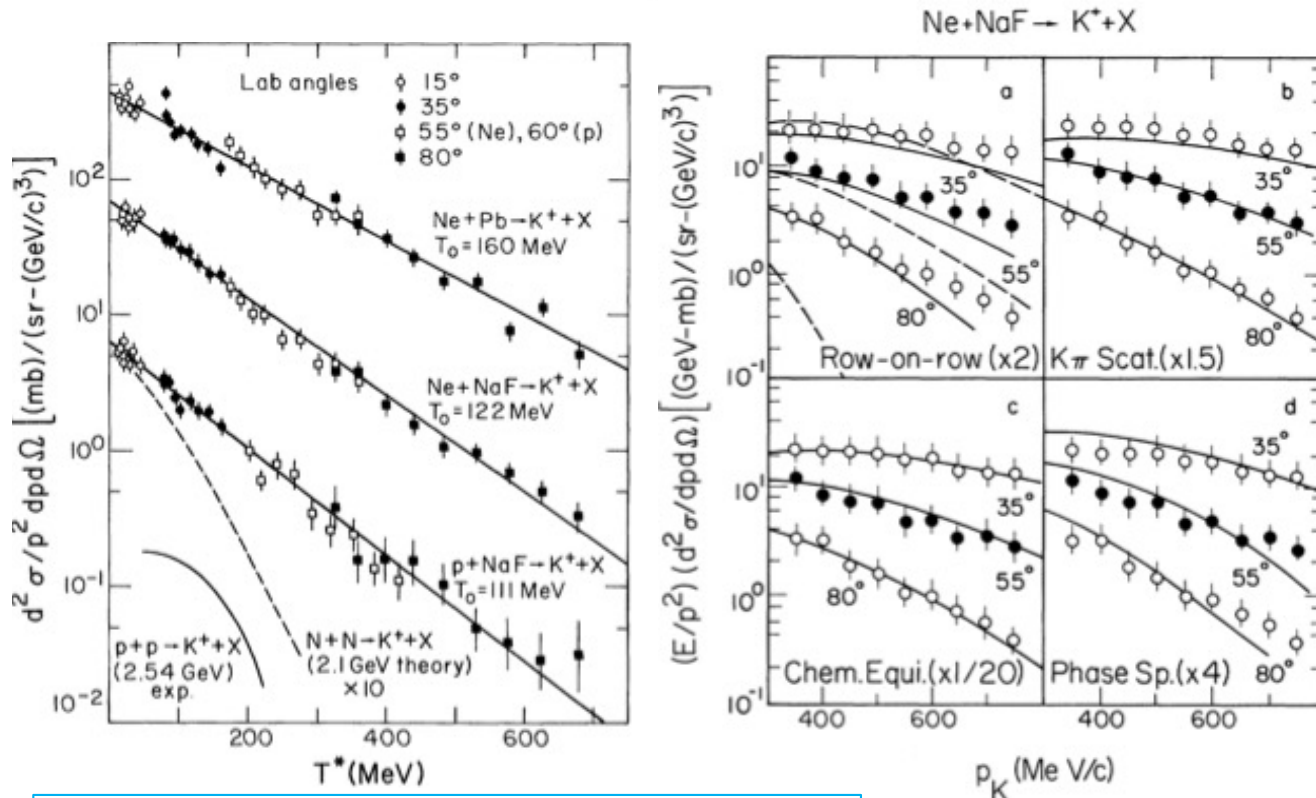
S. Schnetzer,^(a) M.-C. Lemaire,^(b) R. Lombard^(b) E. Moeller,^(c) S. Nagamiya,^(d) G. Shapiro,^(e)
H. Steiner,^(e) and I. Tanihata^(f)

Nuclear Science Division, Lawrence Berkeley Laboratory, University of California, Berkeley, California 94720

(Received 9 June 1982)

PRL 49, 989 (1982)

K^+ meson production by 2.1-GeV/nucleon Ne, d , and p projectiles on NaF and Pb targets has been measured. The cross sections depend exponentially upon the kaon energy in the nucleon-nucleon c.m. frame, with an inverse slope T_0 larger than the values obtained from comparable proton and π^- spectra. The angular distribution in this frame is approximately isotropic. We find that $\sigma(\text{Ne} + \text{Pb} \rightarrow K^+ X) / \sigma(\text{Ne} + \text{NaF} \rightarrow K^+ X) > \sigma(d + \text{Pb} \rightarrow K^+ X) / \sigma(d + \text{NaF} \rightarrow K^+ X)$. Data are compared with theoretical predictions.



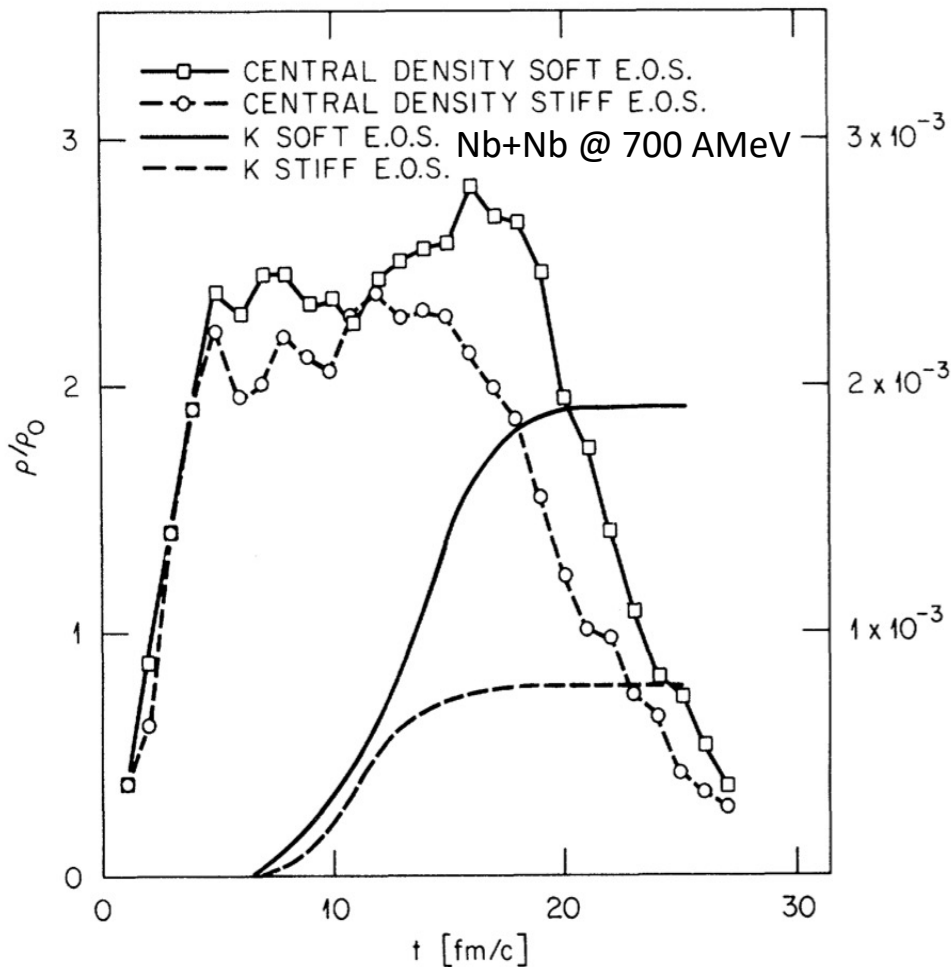
- a) Randrup & Ko, NPA 343, 519 (1980); 411, 537 (1983); Randrup, PLB 99, 9 (1981)
- b) Ko, PRC 23, 2760 (1981)
- c) Asai, Sato & Sano, PLB 98, 19 (1981)
- d) Asai, NPA 365, 519 (1981)

Importance of multiple scattering, strangeness conservation (canonical suppression), and final-state interactions.

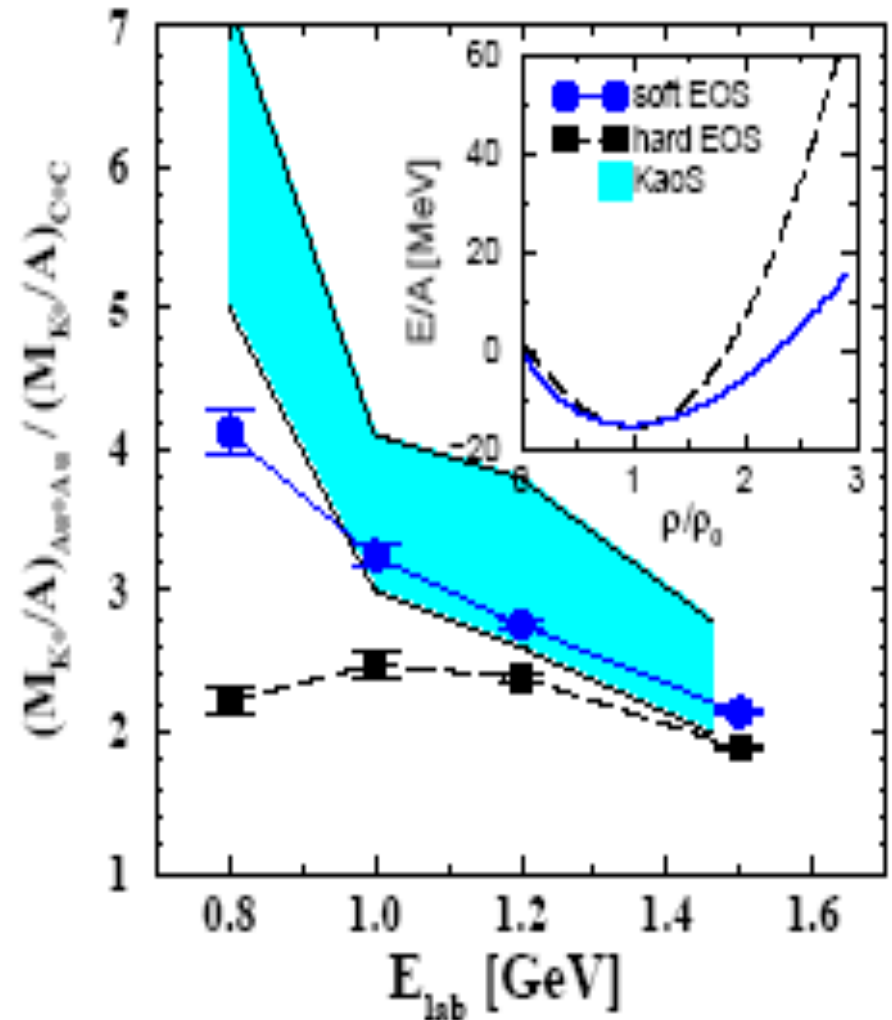
$T^* = K^+$ kinetic energy in NN center of mass

Subthreshold kaon production in high-energy HIC

Aichelin & Ko, PRL 55, 2661 (1985)



Fuchs, PRL 86, 1974 (2001)



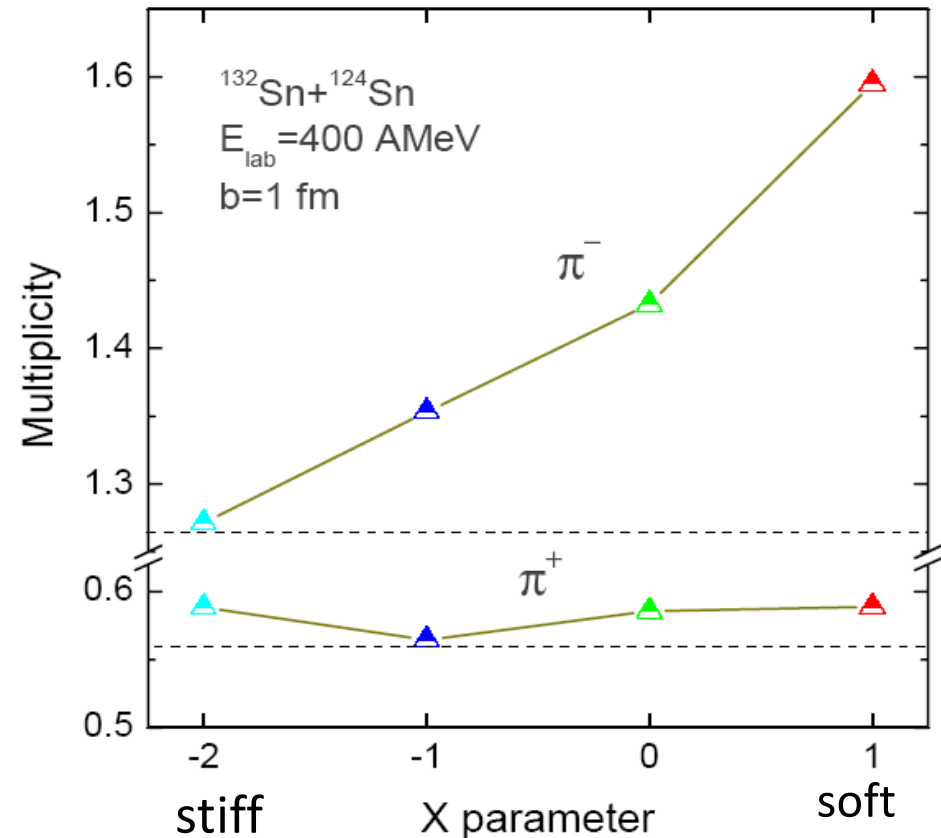
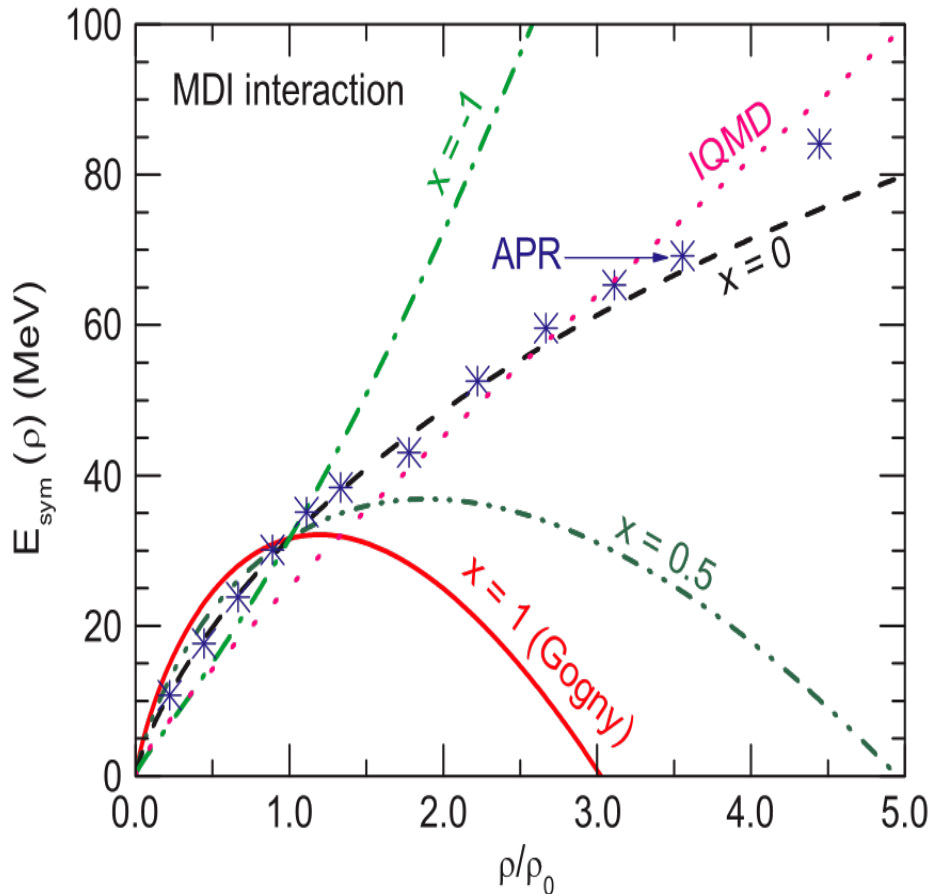
Kaon production at subthreshold energy in HI collisions in BUU models is sensitive to nuclear EOS, and data are consistent with a soft one. 3

Near-threshold pion production

B. A. Li, PRL 88, 192701 (2002)

$$E(\rho, \delta) \approx E(\rho, \delta = 0) + E_{\text{sym}}(\rho)\delta^2, \quad \delta = \frac{\rho_n - \rho_p}{\rho_n + \rho_p}$$

$$E_{\text{sym}}(\rho) \approx S_0 + \frac{L}{3} \left(\frac{\rho - \rho_0}{\rho} \right) + \frac{K_{\text{sym}}}{18} \left(\frac{\rho - \rho_0}{\rho} \right)^2$$



π^- yield in IBUU is sensitive to the symmetry energy $E_{\text{sym}}(\rho)$ since they are mostly produced in the neutron-rich region, with softer one giving more π^- than stiffer one. Difference between π^-/π^+ from super soft ($x = 1$) and super stiff ($x = -1$) $E_{\text{sym}}(\rho)$ is, however, only about 30%, which makes it very challenging to determine $E_{\text{sym}}(\rho)$ from data using transport models.

Pion production in $^{132}\text{Sn} + ^{124}\text{Sn}$ and $^{112}\text{Sn} + ^{108}\text{Sn}$ at 270A MeV and $b = 3$ fm

G. Jhang et al. [$S\pi$ RIT & TMEP], PLB 813, 136016 (2021); H. Wolter et al. [TMEP], PPNP 125, 103962 (2022)

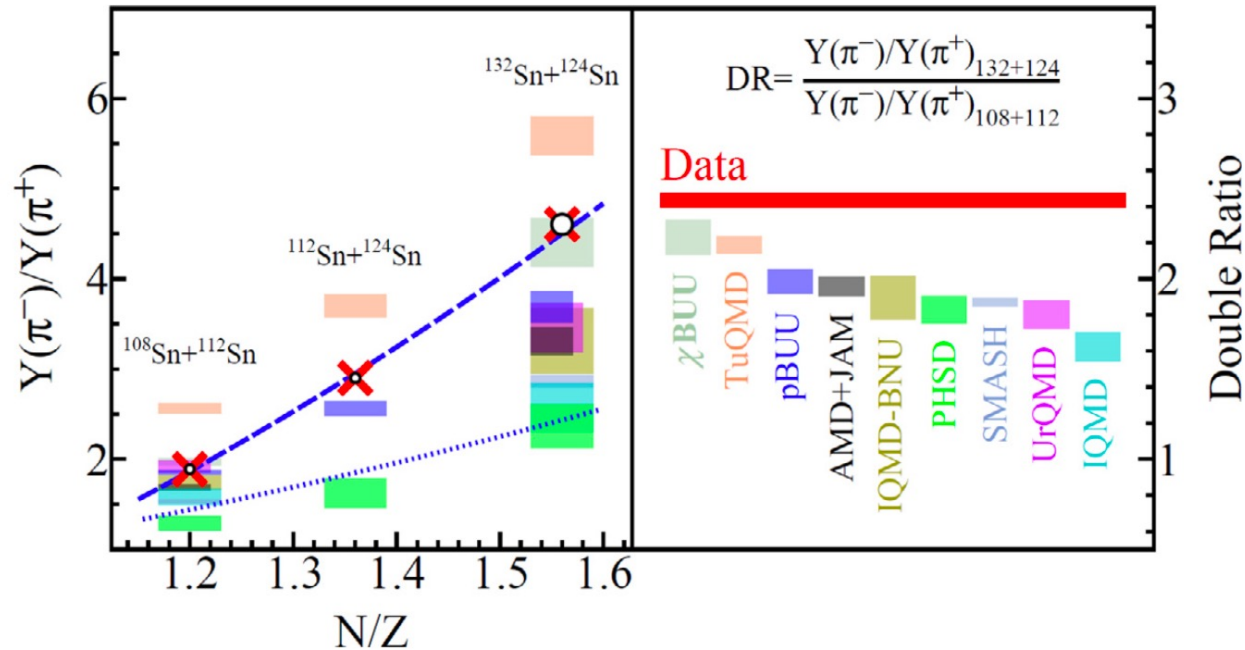
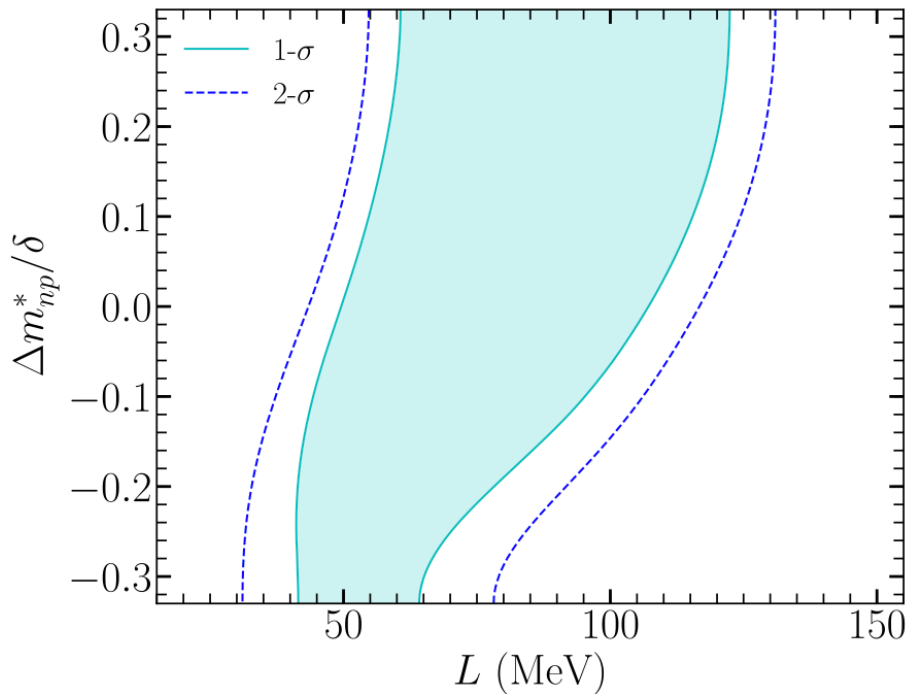


Fig. 13. (Left panel) Charged pion yield ratios as a function of N/Z . The experimental data are shown as crosses with the circles representing the experimental errors. The results of the calculations are represented by colored boxes for the different codes identified by their color in the right panel. The upper and lower boundaries of the boxes give the result for the soft and stiff symmetry energy choices for each code, i.e., the height of the boxes is representative for the sensitivity to the stiffness of the symmetry energy. The dashed blue line is a power-law fit with the function $(N/Z)^{3.6}$, while the dotted blue line represents $(N/Z)^2$ of the system. (Right panel) Double pion yield ratios for $^{132}\text{Sn} + ^{124}\text{Sn}$ and $^{108}\text{Sn} + ^{112}\text{Sn}$. The data and the uncertainty are given by the red horizontal bar, while the results of the transport models are shown by the colored boxes, in a similar way as in the left panel.

Although no transport models can perfectly describe the data yet, the symmetry energy effect in some models is larger than the experimental errors.

Probing the Symmetry Energy with the Spectral Pion Ratio

J. Estee,^{1,2,*} W. G. Lynch^{1,2,†}, C. Y. Tsang,^{1,2} J. Barney,^{1,2} G. Jhang,¹ M. B. Tsang,^{1,2,‡} R. Wang,¹ M. Kaneko, et al. [*SπRIT*]



Correlation contours between L and $\Delta m_{np}^*/\delta$ extracted from the single spectral ratio of the neutron rich $^{132}\text{Sn}+^{124}\text{Sn}$ and near symmetric $^{108}\text{Sn}+^{112}\text{Sn}$ reactions using dcQMD (Dan Cozma). The green shaded region lies within 68% confidence level for data with $p_T > 200$ MeV/c. The dotted blue lines denote contours corresponding to the 95% confidence level.

$$\rightarrow S_0 = 38.3 \pm 4.7 \text{ MeV}, L = 106 \pm 37 \text{ MeV}.$$

- Consistent with $S_0 = (38.29 \pm 4.66)$ MeV and $L = (109.56 \pm 36.41)$ MeV extracted from the PREX-II experiment on neutron skin thickness of Pb, $R_{\text{skin}} = R_n - R_p = (0.29 \pm 0.07)$ fm, using the relativistic mean-field model [Reed, Fattoyev, Horowitz & Piekarewicz, PRL 126, 172503 (2021)].
- Inconsistent with $S_0 = 34.3 \pm 3$ MeV and $L = 58 \pm 19$ MeV based on constraints from neutron star properties (mass, radius, and tidal deformability) and chiral effective theory [Essick, Tews, Landry & Schwenk, PRL 127, 192701 (2021); Yuenhwan Lim & Jeremy Holt, PRL 121, 062701 (2018)].

RVUU with in-medium $NN \leftrightarrow N\Delta$ cross sections

Godbey, Zhang, Ko & Holt, PLB 829, 137134 (2022)

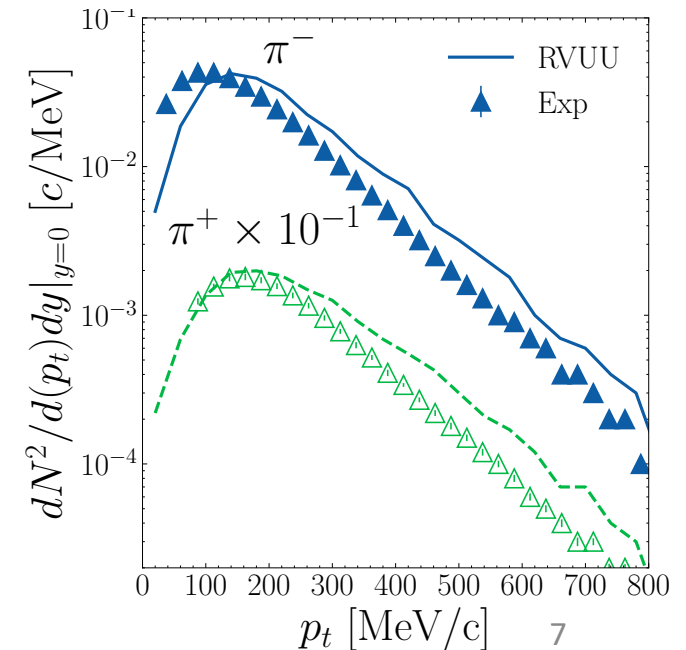
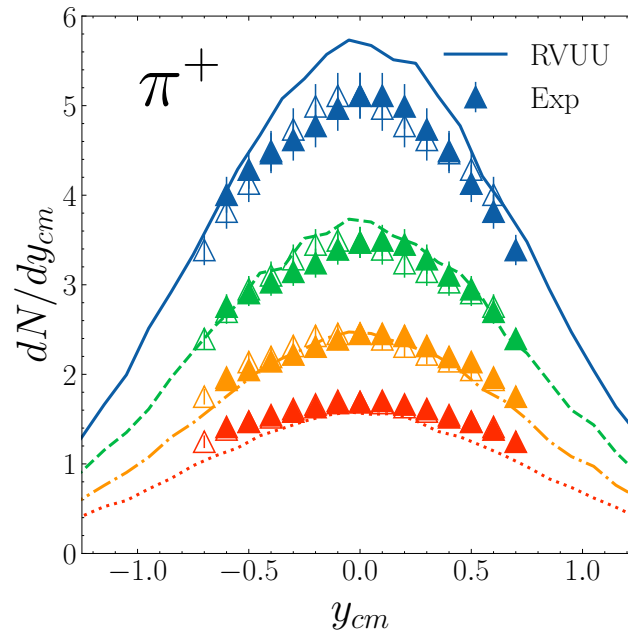
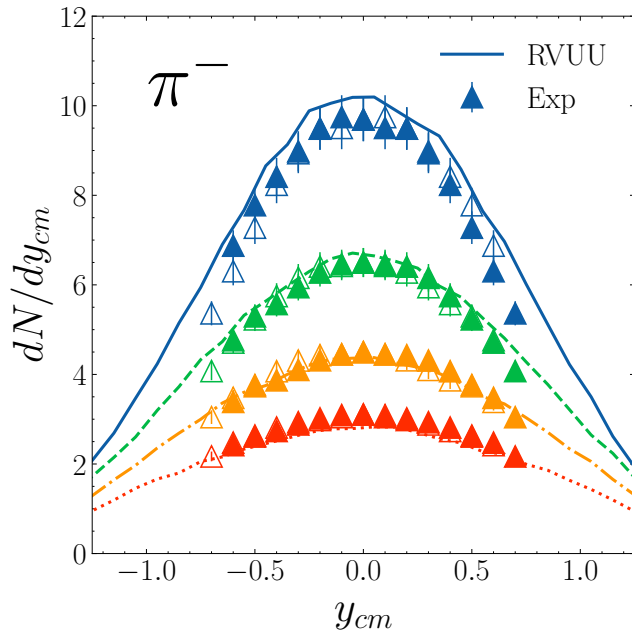
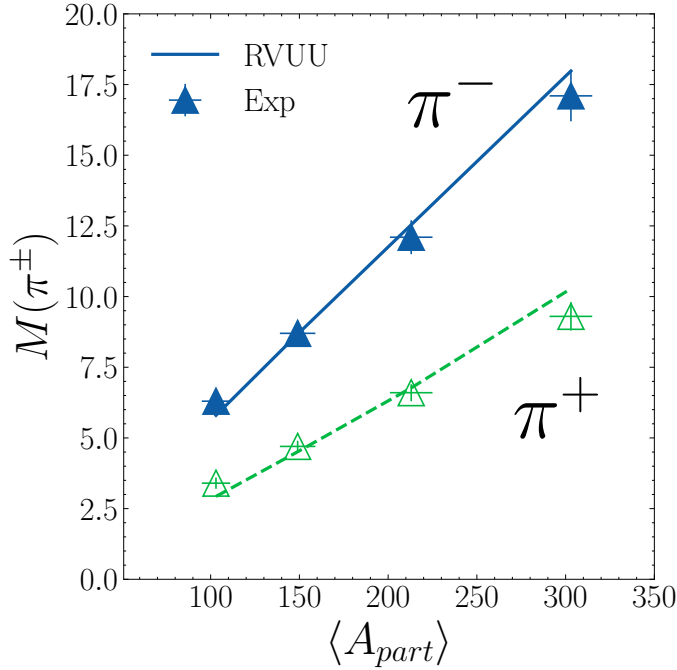
Larionov & Mosel, NPA 728, 135 (2003); Li & Li, PLB 773, 557 (2017); Cui et al., IJMP E30, 2150069 (2021)

$$\sigma_{NN \rightarrow N\Delta}^{med} = \sigma_{NN \rightarrow N\Delta}^{free} e^{-\alpha^\pm (\rho/\rho_0)^{3/2}}$$

Table 1

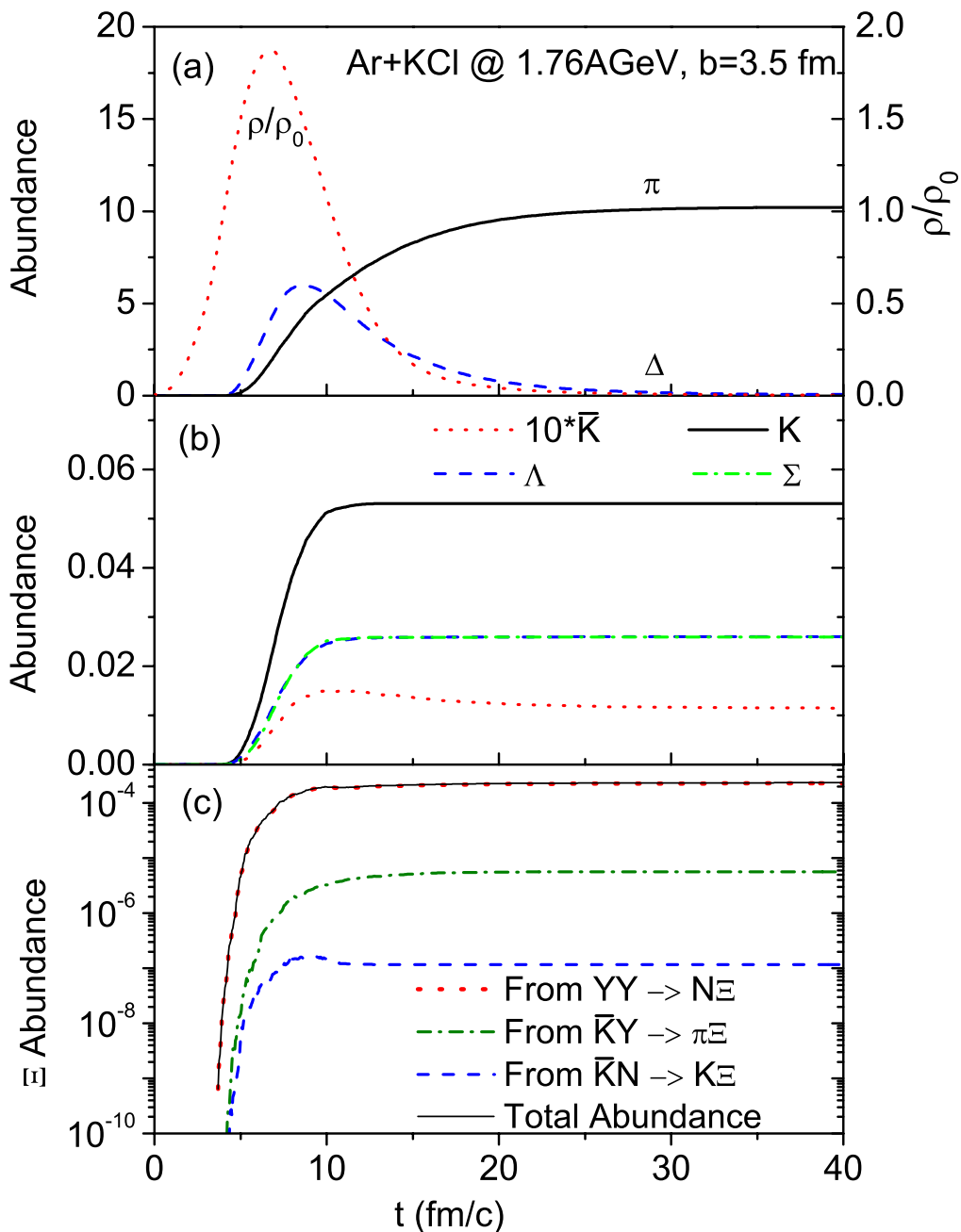
Predicted multiplicities for the 0% – 40% centrality bin from the RVUU model using $\sigma_{NN \rightarrow N\Delta}$ ($\alpha^+ = \alpha^- = 0$) and $\sigma_{NN \rightarrow N\Delta}^*$ with $\alpha^+ = \alpha^- = 0.6$ and with $\alpha^+ = 0.39$ and $\alpha^- = 0.7$ (see Eq. (10)). Experimental results are from Ref. [35].

	$M(\pi^-)$	$M(\pi^+)$
HADES [EPJA 56, 256 (2020)]	$11.1 \pm 0.6 \pm 0.6$	$6.0 \pm 0.3 \pm 0.3$
$\alpha^+ = \alpha^- = 0$	17.2	8.7
$\alpha^+ = \alpha^- = 0.6$	11.8	5.4
$\alpha^+ = 0.39, \alpha^- = 0.7$	11.3	6.2



Deep subthreshold production of Cascade (Ξ)

Li, Chen, Ko & Lee, PRC 85, 064902 (2012)



- Using RVUU with cross sections calculated from meson-exchange model [Li & Ko, NPA 712, 110 (2002)]

$$\sigma(K\bar{K} \Lambda \rightarrow \pi \Xi) \sim 5-10 \text{ mb}$$

$$\sigma(K\bar{K} \Sigma \rightarrow \pi \Xi) \sim 5-10 \text{ mb}$$

$$\sigma(\Lambda \Lambda \rightarrow N \Xi) \sim 40 \text{ mb}$$

$$\sigma(\Lambda \Sigma \rightarrow N \Xi) \sim 40-60 \text{ mb}$$

$$\sigma(\Sigma \Sigma \rightarrow N \Xi) \sim 15-30 \text{ mb}$$

$$\sigma(KN \rightarrow K\bar{K} \Xi) \sim 0.2 \text{ mb}$$

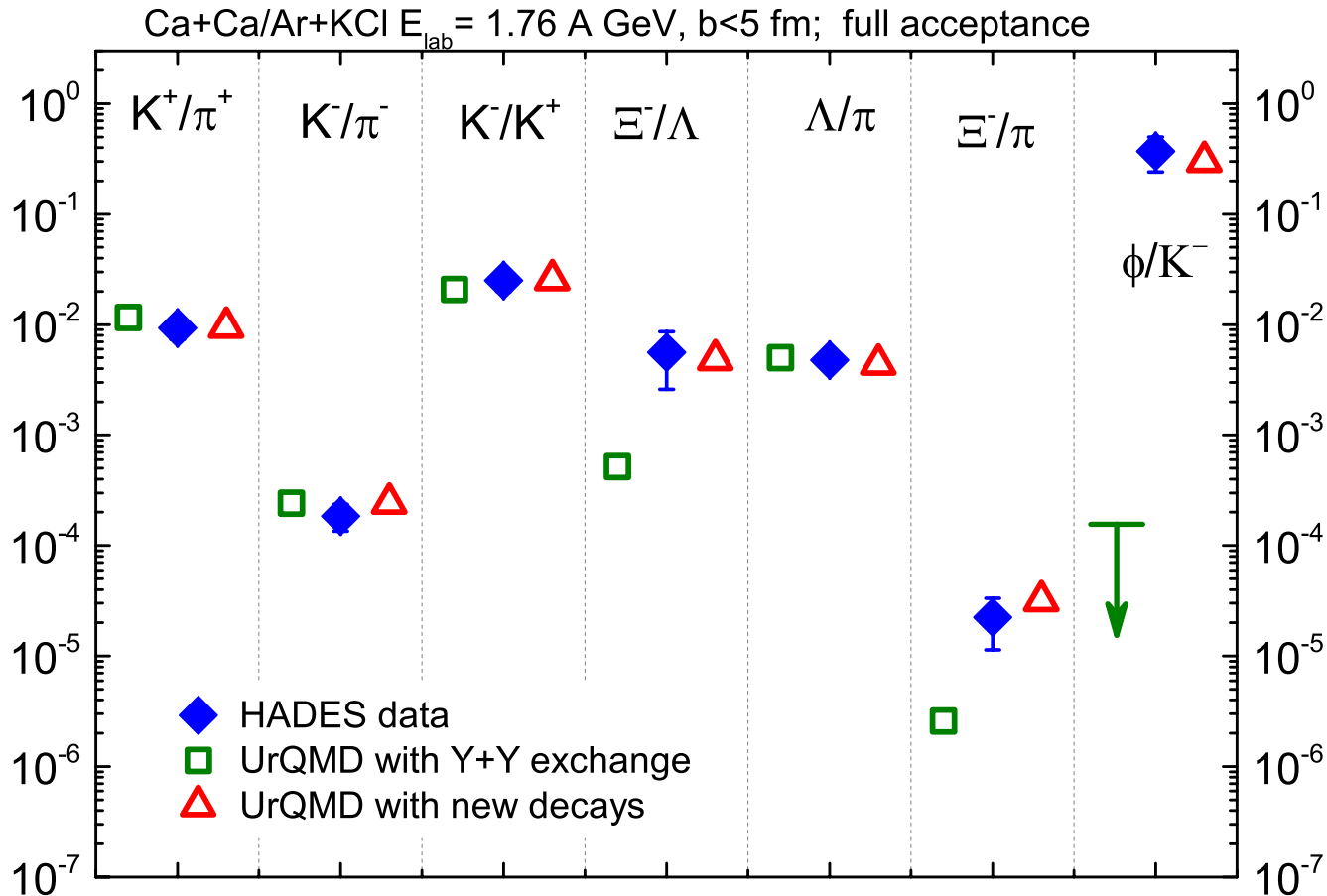
$$\rightarrow \Xi^- / (\Lambda + \Sigma^0) \sim 3.4 \times 10^{-3}$$

compared with HADES data of 5.6×10^{-3} [Agakishiev et al., PRL 103, 132301 (2009)]

- Similar conclusions from UrQMD [Graef, Steiheimer, Li & Bleicher, PRC 90, 064909 (2014)]

Role of heavy baryonic resonances

J. Steiheimer and M. Bleicher, J. Phys. G43, 015104 (2016)



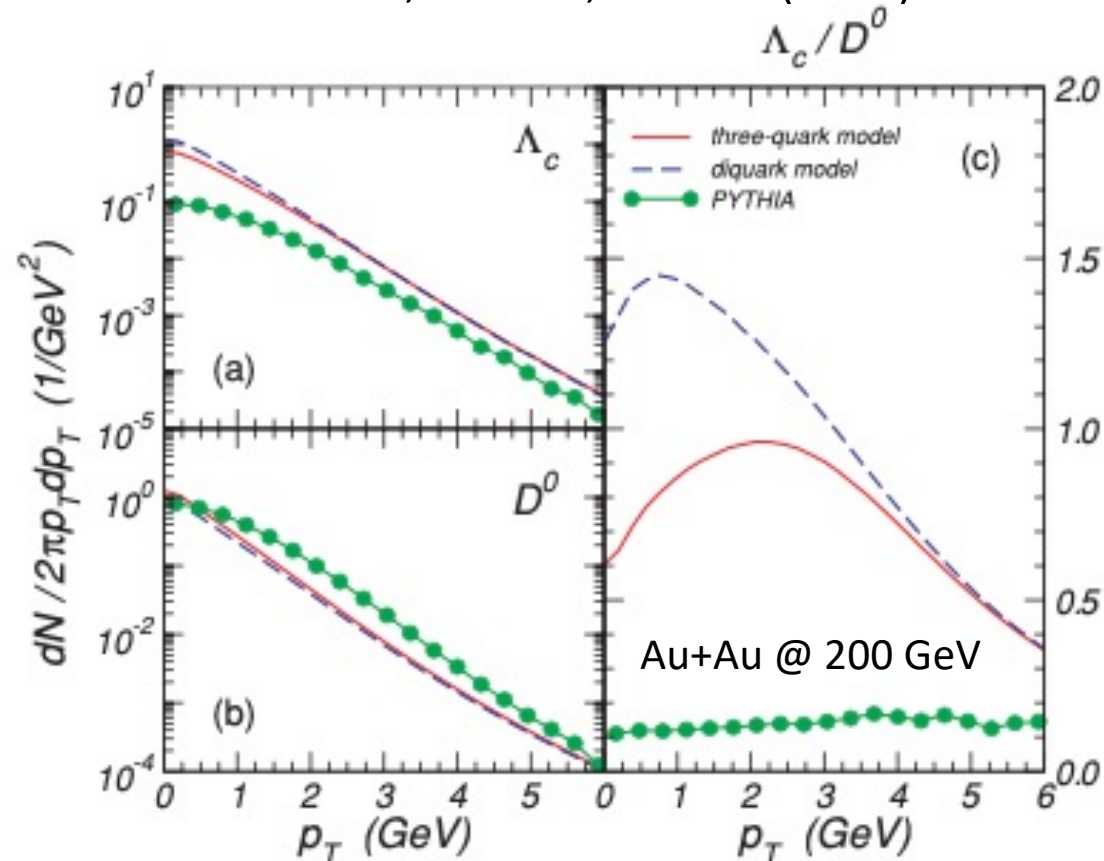
Good agreement with data after including in UrQMD decays of $N^*(1990)$, $N^*(2080)$, $N^*(2190)$, $N^*(2220)$, and $N^*(2250)$ to ΞKK with a branching ratio of 10% and to $N\phi$ with a BR of 0.2%.

Λ_c Enhancement from Strongly Coupled Quark-Gluon Plasma

Su Houn Lee,¹ Kazuaki Ohnishi,¹ Shigehiro Yasui,^{1,2} In-Kwon Yoo,³ and Che Ming Ko⁴

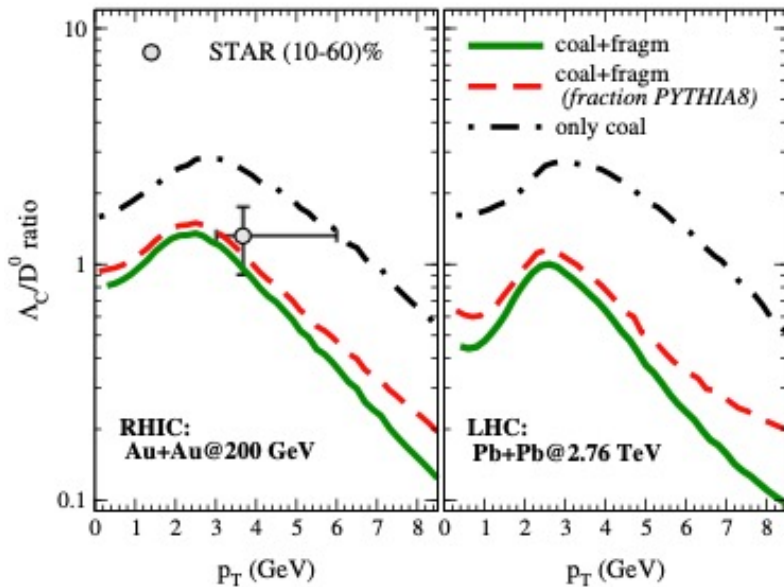
We propose the enhancement of Λ_c as a novel quark-gluon plasma signal in heavy ion collisions at the BNL Relativistic Heavy Ion Collider and the CERN Large Hadron Collider. Assuming a stable bound diquark state in the strongly coupled quark-gluon plasma near the critical temperature, we argue that the direct two-body collision between a c quark and a $[ud]$ diquark would lead to an enhanced Λ_c production in comparison with the normal three-body collision among independent c , u , and d quarks. In the coalescence model, we find that the Λ_c/D yield ratio is enhanced substantially due to the diquark correlation.

Oh et al., PRC 79, 044905 (2009)



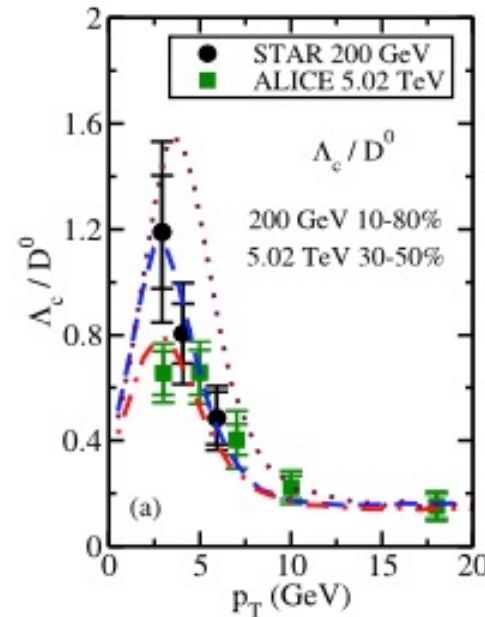
Λ_c to D^0 ratio in experiments and models

Plumari et al., EPJC 78, 348 (2018)



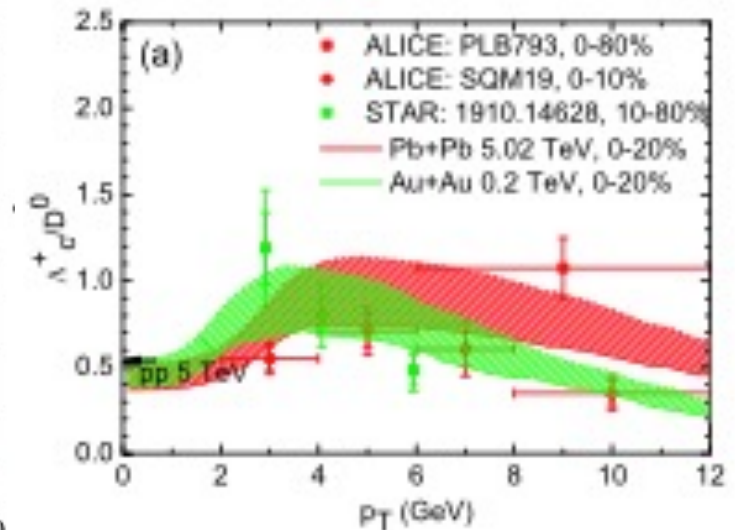
Coalescence model with contribution of known resonances and renormalized coalescence probability of unity for zero momentum charm quarks.

Cao et al., PLB 807, 135561 (2020);
Cho et al., PRC 101, 024909 (2020)



Coalescence model with contribution from known resonances and including the flow effect.

He & Rapp, PRL 124, 042301 (2020)



Energy conserving coalescence model with contributions from known and also missing resonances.

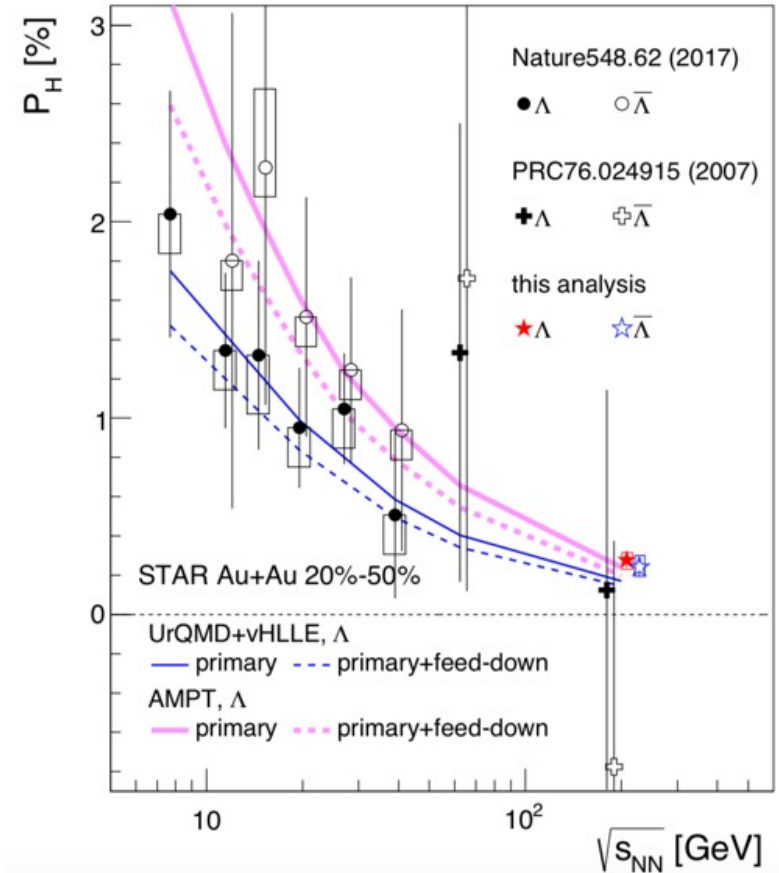
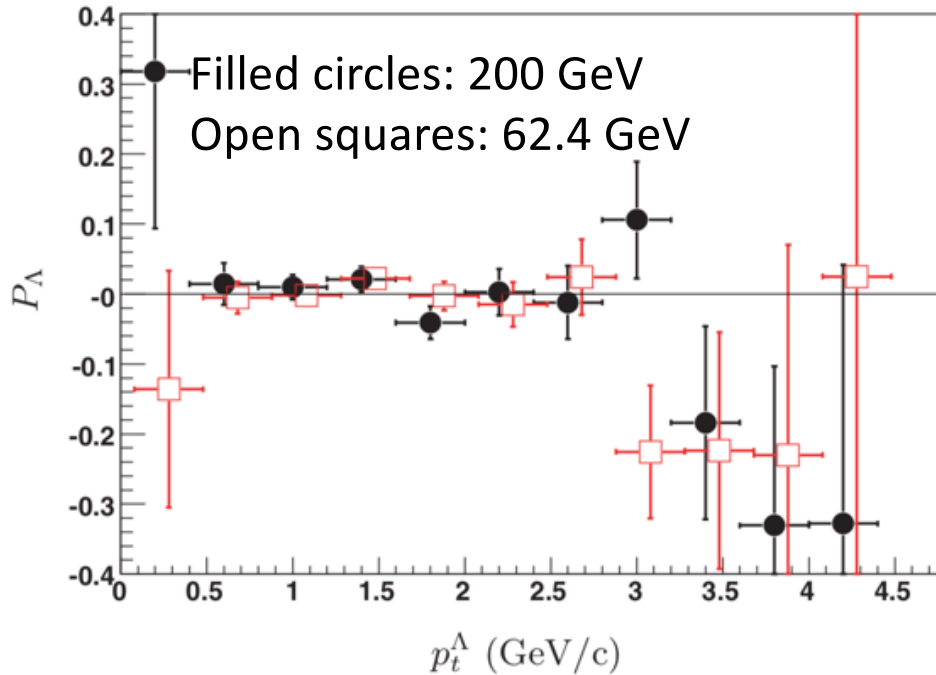
No evidence for diquarks in QGP!

Λ polarization in relativistic heavy ion collisions

- First suggested by Z. T. Liang & X. N. Wang, PRL 94, 102301 (2005)

Abelev (STAR), PRC 76, 024915 (2007)

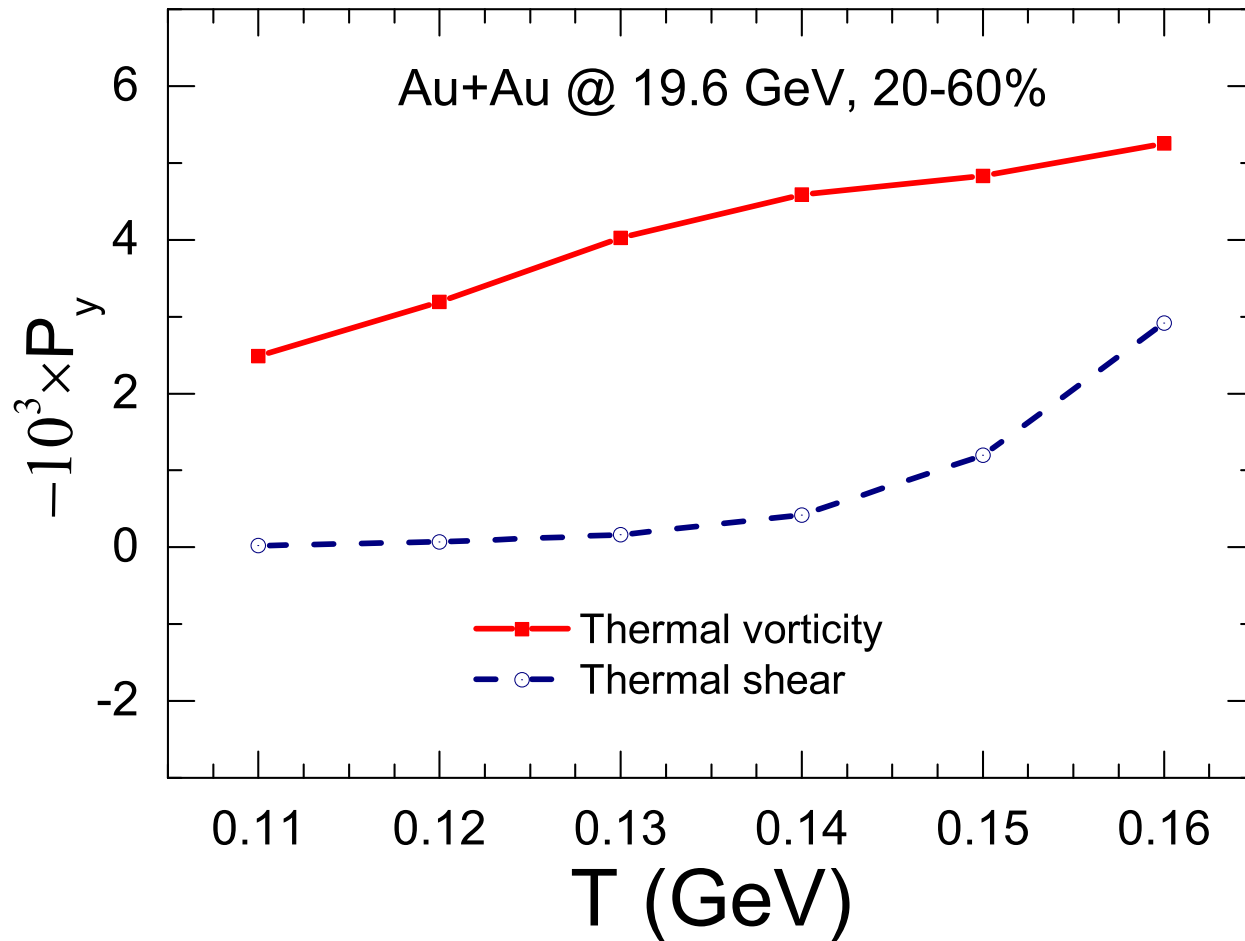
Adam (STAR), PRC 98, 14910 (2018)



- Studies based on fluid dynamics [Cernai, Becattini, Karpenko, Voloshin] and transport models [Wang et al.] assuming Λ in thermal equilibrium in the rotating fireball at chemical freeze out of HIC both predict Λ polarizations comparable to the STAR data.

Evolution of Λ global polarization during hadronic expansion

Yifeng Sun, Zhen Zhang, Wenbin Zhao & Ko, PRC 105, 034911 (2022)



MUSIC+UrQMD: Lambda global polarization due to thermal vorticity decreases with decreasing spin decoupling temperature, and that due to thermal shear is less important.

Spin polarization vector of a fermion

- Shuai Liu & Yi Yin, JHEP 07, 188 (2021)
- F. Becattini, M. Buzzegoli & A. Palermo, PLB 820, 136519 (2021)
- Cong Yi, Shi Pu & Di-Lun Yang, PRC 104, 064901 (2021)

$$S^\mu(x, p) = -\frac{1}{8m}(1 - n_F)\epsilon^{\mu\nu\rho\sigma}p_\nu\varpi_{\rho\sigma}(x) - \frac{1}{4m}(1 - n_F)\epsilon^{\mu\nu\rho\sigma}p_\nu\frac{n_\rho p^\lambda \xi_{\lambda\sigma}(x)}{n \cdot p}$$

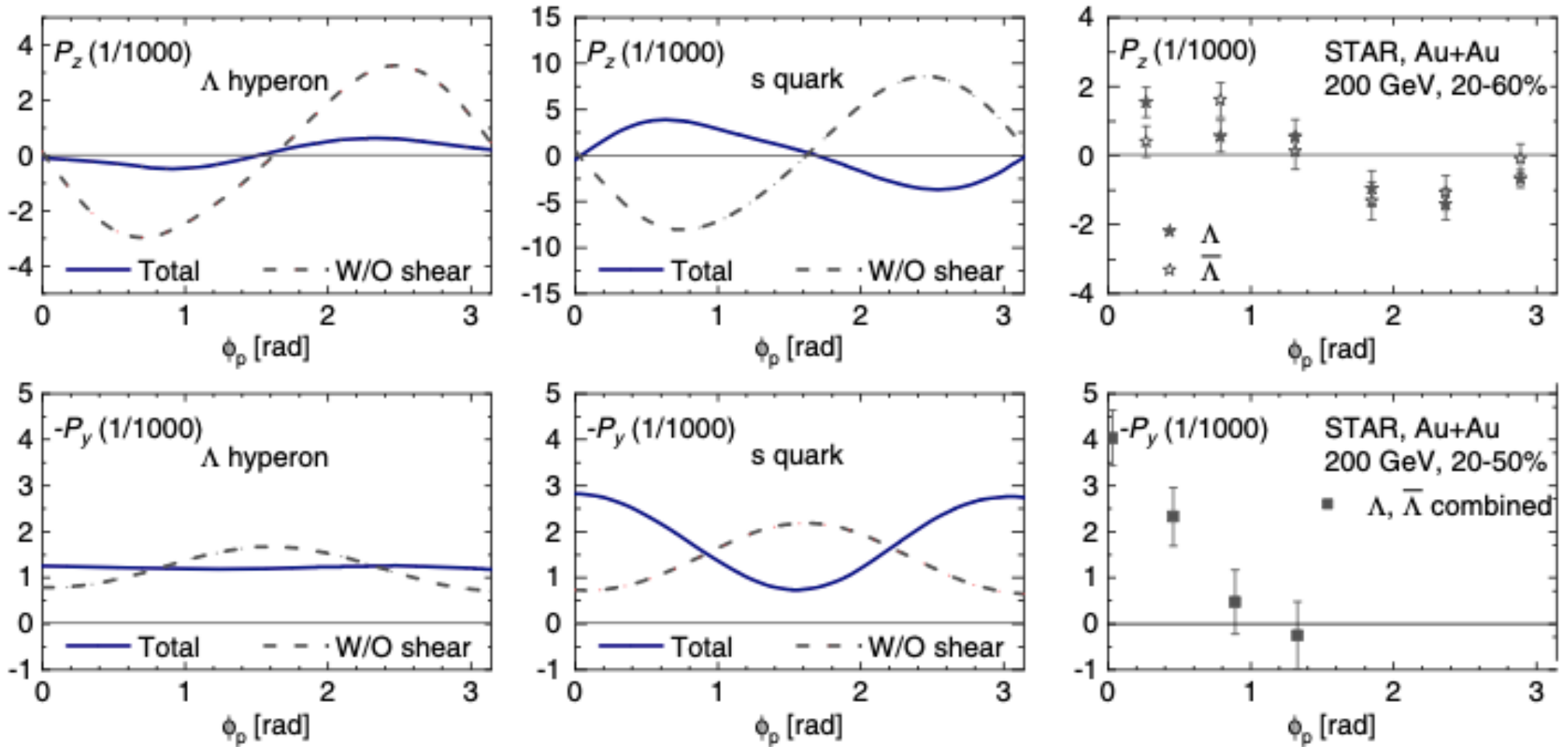
where p is the 4-momentum of the fermion, n_F is the Fermi-Dirac distribution function, n is a unit four vector that specifies the frame of reference, and

$$\text{thermal vorticity } \varpi_{\rho\sigma} = \frac{1}{2}(\partial_\sigma\beta_\rho - \partial_\rho\beta_\sigma)$$
$$\text{thermal shear } \xi_{\rho\sigma} = \frac{1}{2}(\partial_\sigma\beta_\rho + \partial_\rho\beta_\sigma)$$

where $\beta = u/T$ with u being the flow field.

Effects of thermal shear on local spin polarizations

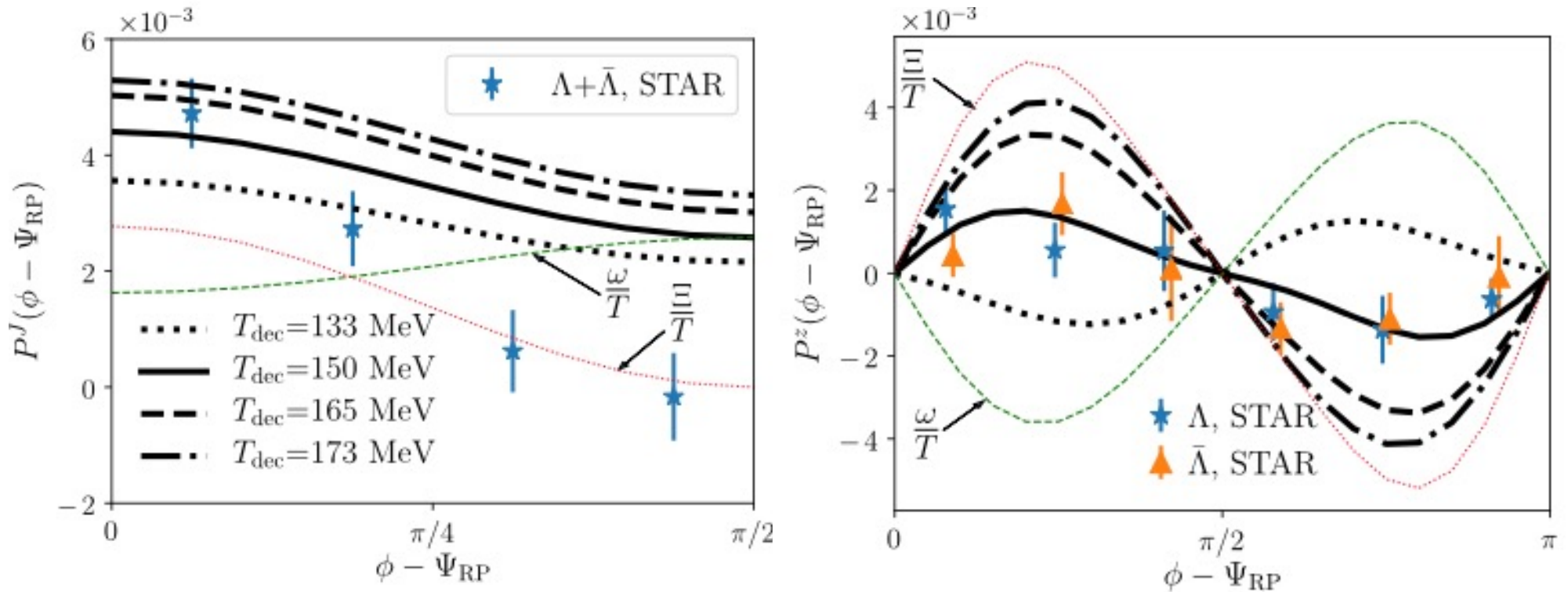
Baochi Fu, Shuai Y. F. Liu, Longgang Pang, Huichao Song, and Yi Yin, PRL 127, 142301 (2021)



- 3+1 MUSIC: including the thermal shear contribution, s quarks show similar local spin polarization as in experiments for Λ , but not Λ s.
- Will Λ have same local spin polarization as s quark if it is produced from quark coalescence?

Local polarization and isothermal local equilibrium in HIC

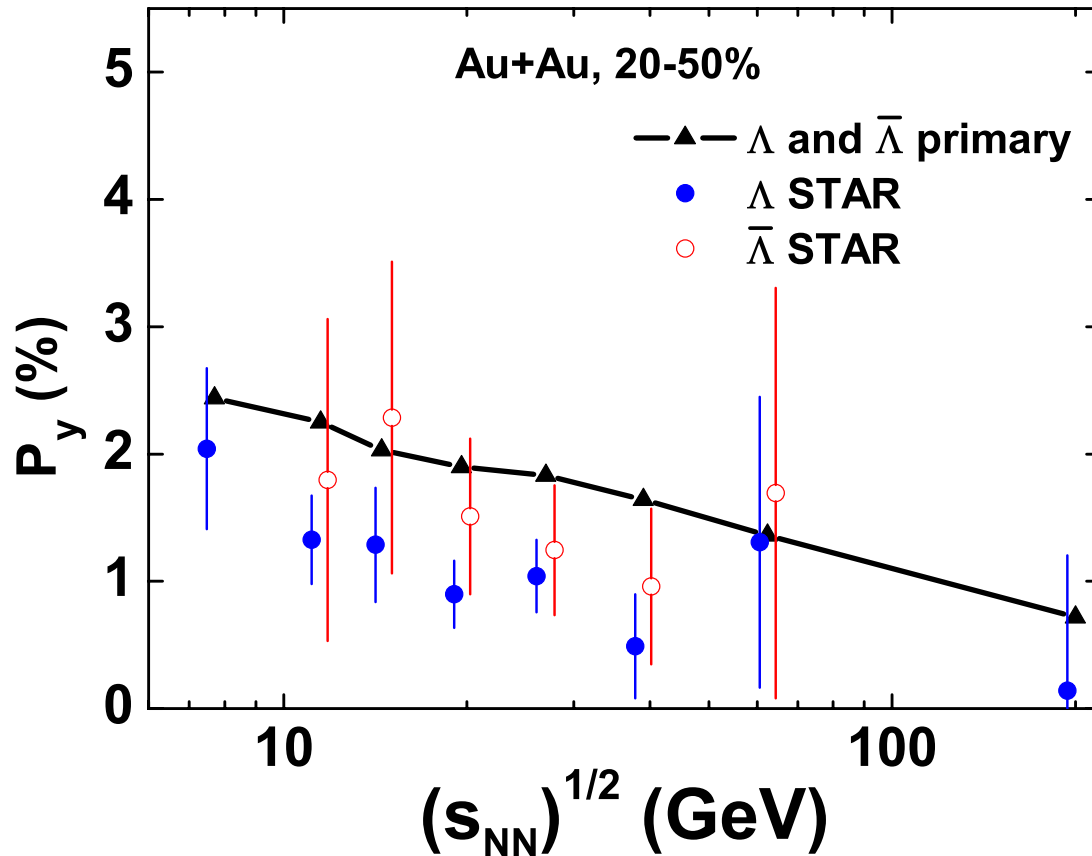
F. Becattini, M. Buzzegoli, and A. Palermo, G. Inghirami, and I. Karpenko, PRL 127, 272302 (2021)



3+1 viscos hydro (eHLE & EVHO-QGP): Data is consistent with “isothermal local equilibrium” ($\partial\beta \rightarrow \frac{1}{T_{dec}}\partial u$) of Λ spin polarization in thermal vorticity and shear fields at temperature of 150 MeV . 16

Kinetic approach to Lambda polarization in heavy ion collisions

Yifeng Sun and CMK, PRC 96, 024906 (2017)



- Quarks follow chiral vortical equations of motion

$$\dot{\mathbf{x}} = \frac{1 + \lambda \frac{\boldsymbol{\omega}}{p}}{1 + 3\lambda \frac{\boldsymbol{\omega}}{p} \cdot \hat{\mathbf{p}}}$$

$$\dot{\mathbf{p}} = 0$$

$$\boldsymbol{\omega} = \frac{1}{2} \nabla \times \mathbf{v}$$

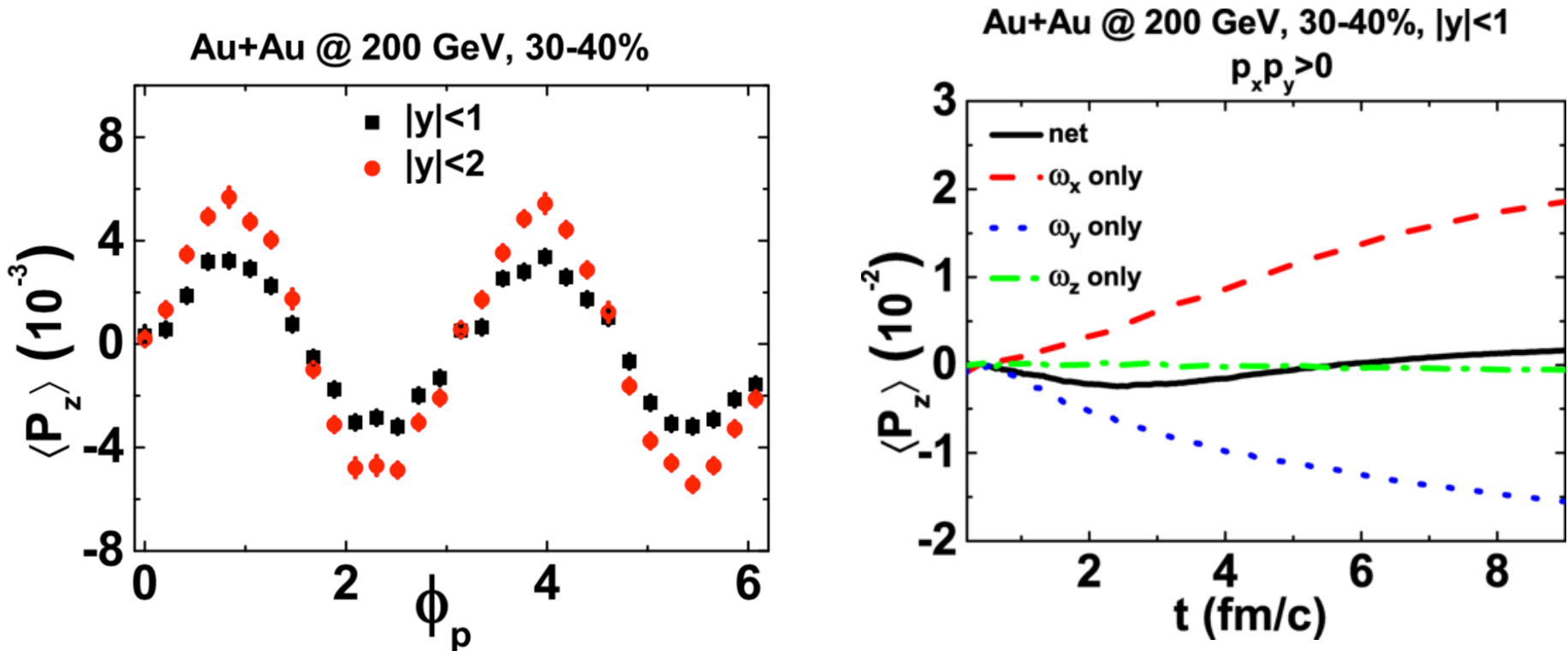
$$\lambda : \text{ helicity} = \pm 1$$

$$\mathbf{v} : \text{ velocity field}$$

- Quarks and antiquarks of opposite helicities undergo helicity flip scattering.
- Polarized Lambda formed from polarized quarks via coalescence.
- Lambda polarization decreases with energy due to decreasing vorticity.
- Similar to results based on statistical model based on vorticity from hydro or transport model at T_C .
- Seemingly larger Lambda than anti-Lambda polarizations in data is not understood.

■ Azimuthal angle dependence of longitudinal spin polarization

Yifeng Sun & CMK, PRC 99, 011903 (R) (2019)



- Similar to that from preliminary STAR data [Niida, NPA (2018)].
- Opposite sign from those based on thermal-vorticity [Becattini & Karpenko, PRL 120, 012302 (2018); Xia et al., PRC 98, 024905 (2018)].
- Similar results are obtained from a covariant angular-momentum conserved transport approach via side jumps in quark-quark scatterings to take into account the spin-orbit interactions (Shuai Liu, Yiefeng Sun & CMK, PRL 125, 062301 (2020)).

Exotic mesons, baryons and dibaryons

Cho, Furumoto, Hyodo, Jido, Ko, Lee, Nielsen, Ohnishi, Sekihara, Yasui, and Yazaki [ExHIC Collaboration], PRL 106, 212001 (2011); PRC 84, 064910 (2011); PPNP 95, 279 (2017)

Particle	m (MeV)	g	I	J^P	$2q/3q/6q$	$4q/5q/8q$	Mol.	$\omega_{\text{Mol.}}$ (MeV)	Decay mode
Mesons									
$f_0(980)$	980	1	0	0^+	$q\bar{q}, s\bar{s}(L=1)$	$q\bar{q}s\bar{s}$	$\bar{K}K$	67.8(B)	$\pi\pi$ (Strong decay)
$a_0(980)$	980	3	1	0^+	$q\bar{q}(L=1)$	$q\bar{q}s\bar{s}$	$\bar{K}K$	67.8(B)	$\eta\pi$ (Strong decay)
$K(1460)$	1460	2	1/2	0^-	$q\bar{s}$	$q\bar{q}q\bar{s}$	$\bar{K}KK$	69.0(R)	$K\pi\pi$ (Strong decay)
$D_s(2317)$	2317	1	0	0^+	$c\bar{s}(L=1)$	$q\bar{q}c\bar{s}$	DK	273(B)	$D_s\pi$ (Strong decay)
T_{cc}^{1a}	3797	3	0	1^+	—	$qqc\bar{c}$	$\bar{D}\bar{D}^*$	476(B)	$K^+\pi^- + K^+\pi^- + \pi^-$
$X(3872)$	3872	3	0	$1^+, 2^-^c$	$c\bar{c}(L=2)$	$q\bar{q}c\bar{c}$	$\bar{D}\bar{D}^*$	3.6(B)	$J/\psi\pi\pi$ (Strong decay)
$Z^+(4430)^b$	4430	3	1	0^-^c	—	$q\bar{q}c\bar{c}(L=1)$	$D_1\bar{D}^*$	13.5(B)	$J/\psi\pi$ (Strong decay)
T_{cb}^{0a}	7123	1	0	0^+	—	$qqc\bar{b}$	$\bar{D}B$	128(B)	$K^+\pi^- + K^+\pi^-$
Baryons									
$\Lambda(1405)$	1405	2	0	$1/2^-$	$qqqs(L=1)$	$qqqs\bar{q}$	$\bar{K}N$	20.5(R)–174(B)	$\pi\Sigma$ (Strong decay)
$\Theta^+(1530)^b$	1530	2	0	$1/2^+^c$	—	$qqqq\bar{s}(L=1)$	—	—	KN (Strong decay)
$\bar{K}KN^a$	1920	4	1/2	$1/2^+$	—	$qqqs\bar{s}(L=1)$	$\bar{K}KN$	42(R)	$K\pi\Sigma, \pi\eta N$ (Strong decay)
$\bar{D}N^a$	2790	2	0	$1/2^-$	—	$qqqq\bar{c}$	$\bar{D}N$	6.48(R)	$K^+\pi^-\pi^- + p$
\bar{D}^*N^a	2919	4	0	$3/2^-$	—	$qqqq\bar{c}(L=2)$	\bar{D}^*N	6.48(R)	$\bar{D} + N$ (Strong decay)
Θ_{cs}^a	2980	4	1/2	$1/2^+$	—	$qqqs\bar{c}(L=1)$	—	—	$\Lambda + K^+\pi^-$
BN^a	6200	2	0	$1/2^-$	—	$qqqq\bar{b}$	BN	25.4(R)	$K^+\pi^-\pi^- + \pi^+ + p$
B^*N^a	6226	4	0	$3/2^-$	—	$qqqq\bar{b}(L=2)$	B^*N	25.4(R)	$B + N$ (Strong decay)
Dibaryons									
H^a	2245	1	0	0^+	$qqqqss$	—	ΞN	73.2(B)	$\Lambda\Lambda$ (Strong decay)
$\bar{K}NN^b$	2352	2	1/2	0^-^c	$qqqqqs(L=1)$	$qqqqq\bar{s}$	$\bar{K}NN$	20.5(T)–174(T)	ΛN (Strong decay)
$\Omega\Omega^a$	3228	1	0	0^+	$ssssss$	—	$\Omega\Omega$	98.8(R)	$\Lambda K^- + \Lambda K^-$
H_c^{++a}	3377	3	1	0^+	$qqqqsc$	—	$\Xi_c N$	187(B)	$\Lambda K^-\pi^+\pi^+ + p$
$\bar{D}NN^a$	3734	2	1/2	0^-	—	$qqqqq\bar{q}$	$\bar{D}NN$	6.48(T)	$K^+\pi^- + d, K^+\pi^-\pi^- + p + p$
BNN^a	7147	2	1/2	0^-	—	$qqqqq\bar{q}$	BNN	25.4(T)	$K^+\pi^- + d, K^+\pi^- + p + p$

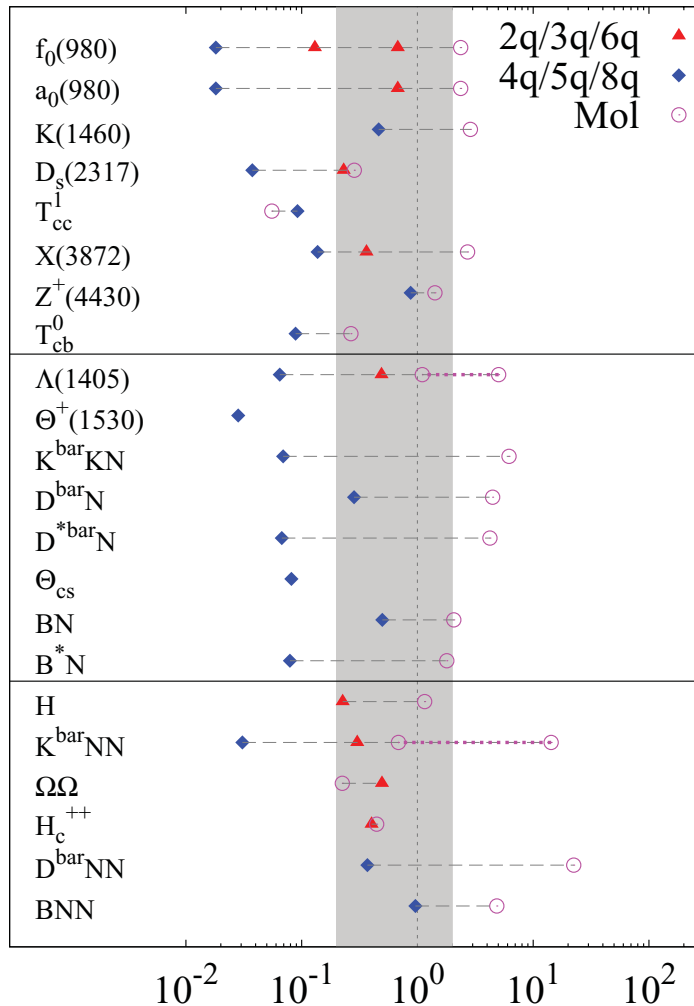
^aParticles that are newly predicted by theoretical models.

^bParticles that are not yet established.

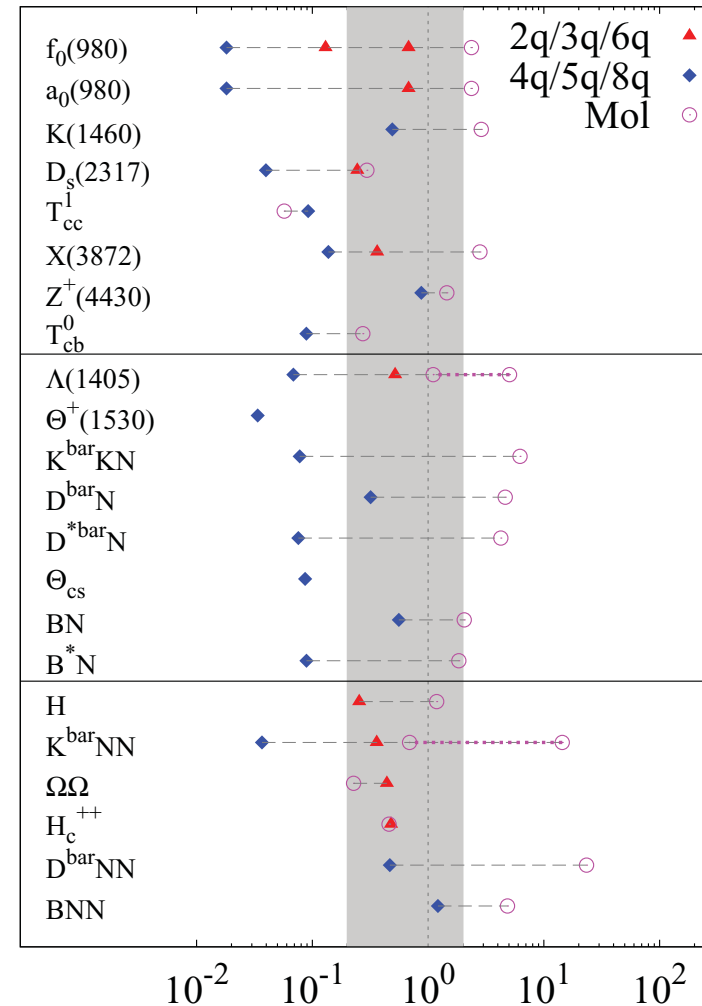
^cUndetermined quantum numbers of existing particles.

Ratio of exotic hadron yields from coalescence and statistical models

Coalescence / Statistical model ratio at RHIC



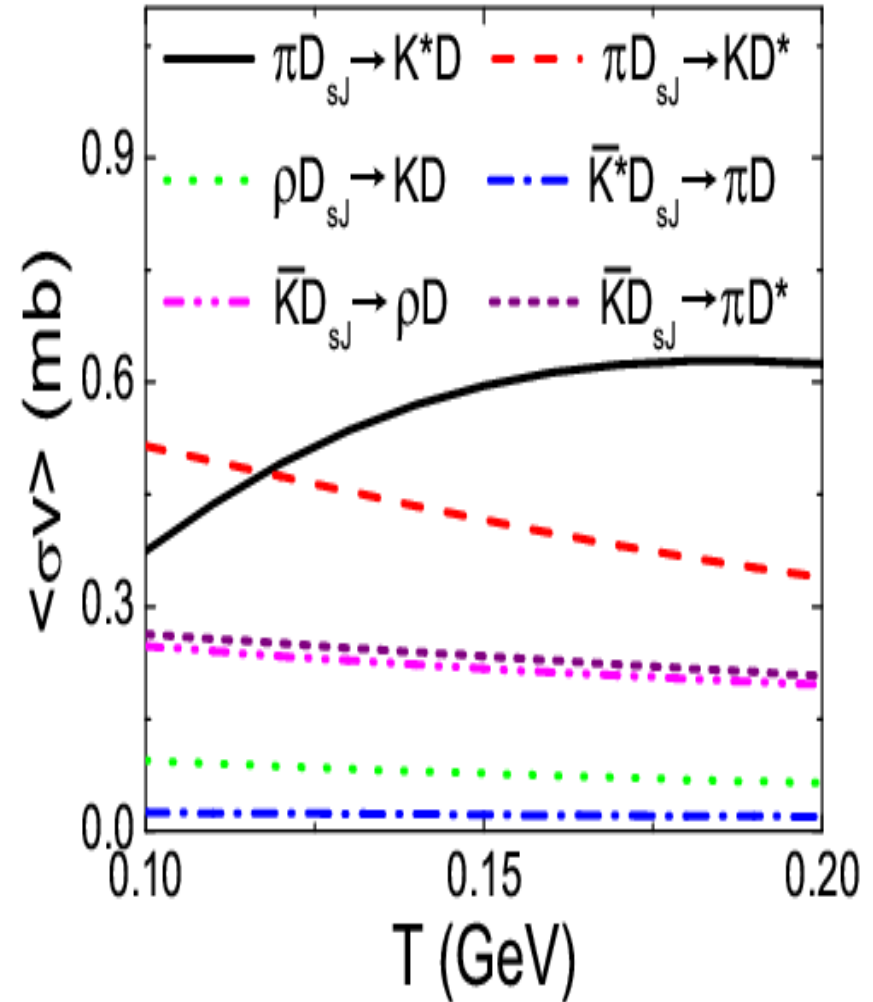
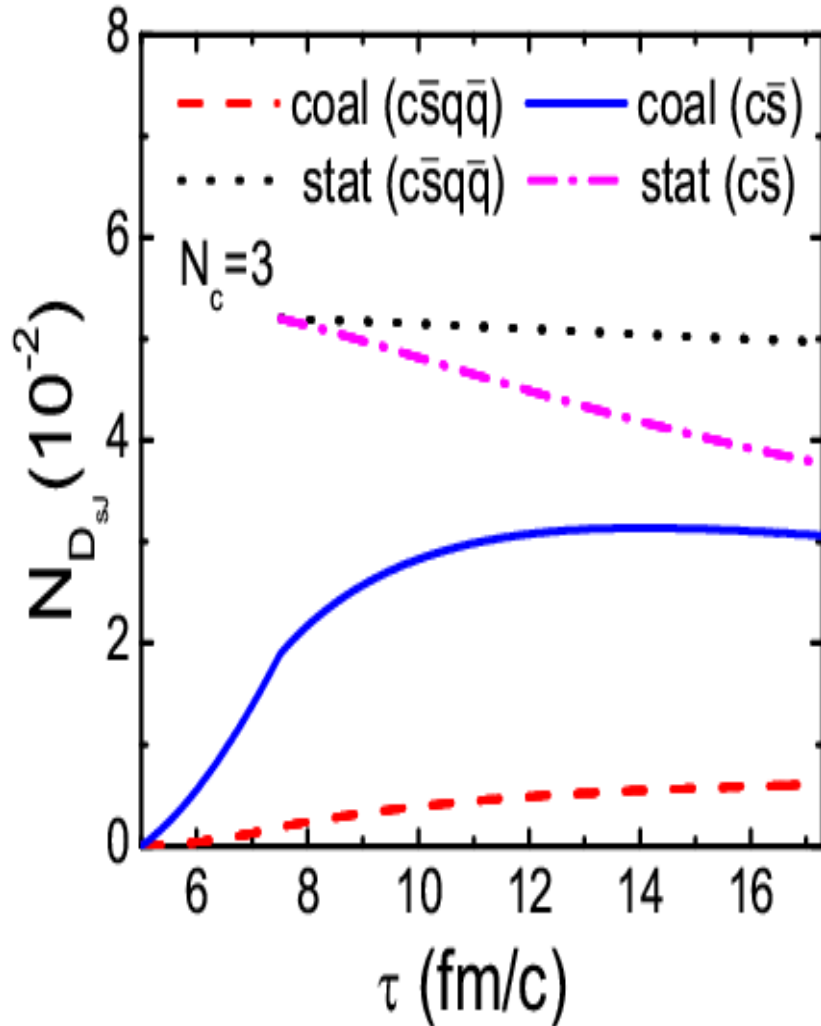
Coalescence / Statistical model ratio at LHC



Multiquark hadrons are suppressed while hadronic molecules are enhanced in coalescence model, compared to the statistical model predictions.

$D_{sJ}(2317)$ production at RHIC

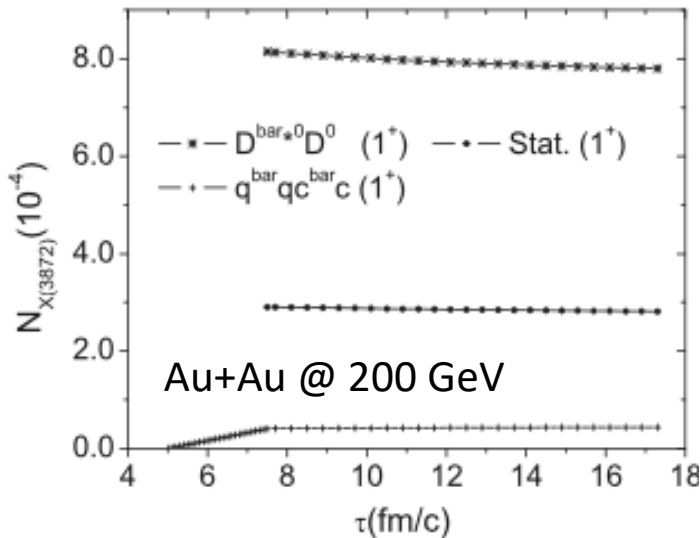
Chen, Liu, Nielsen & Ko, PRC 76, 064903 (2007)



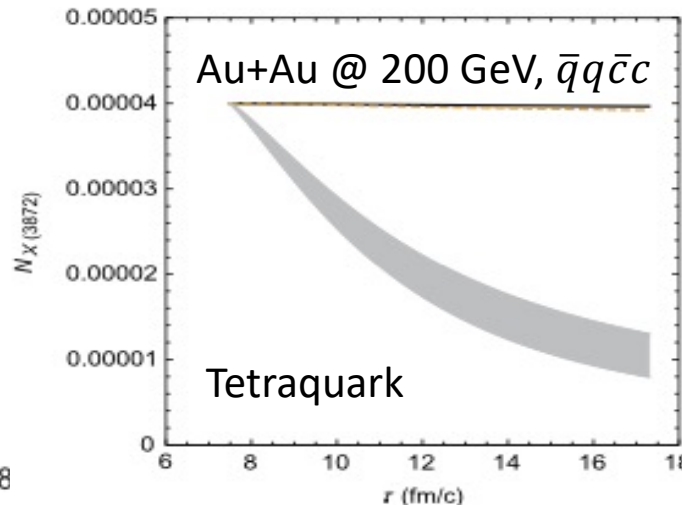
- Cross sections for strangeness-exchange reactions are for four-quark state and are larger by ~ 9 for two-quark state.
- Final yield is sensitive to the quark structure of $D_{sJ}(2317)$.

X(3872) production in HIC

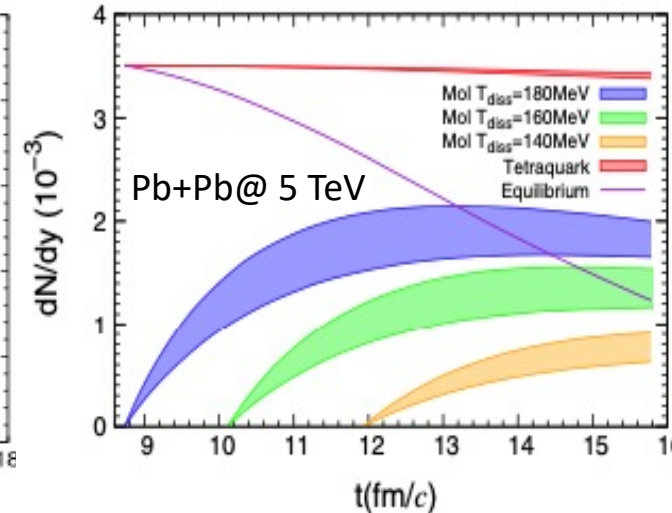
Cho & Lee, PRC 88, 054901 (2013)



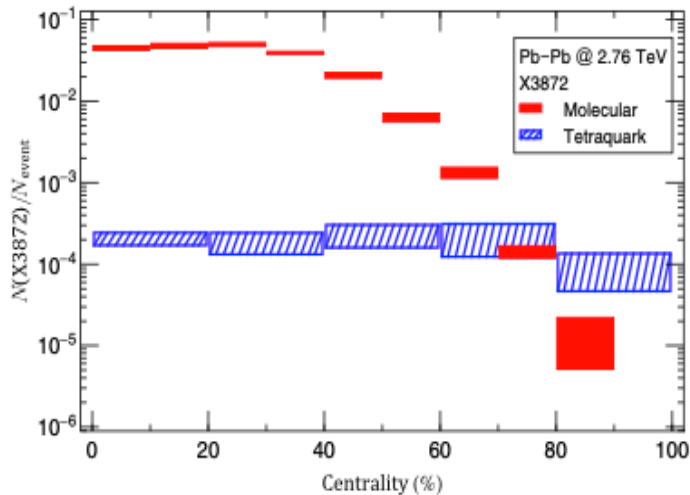
Abreu et al., PLB 761, 303 (2016)



Wu, Du, Sibila & Rapp, EPJA 57, 122 (2021)



Hui Zhang et al, PRL 136, 012301 (2021)



- Cho & Lee use kinetic approach with initial numbers from coalescence model and include $\pi(\rho)X \leftrightarrow D\bar{D}, D^*\bar{D}, D^*\bar{D}^*$ reactions.
- Abreu et al. include anomalous vertices in $\pi X \leftrightarrow D\bar{D}, D^*\bar{D}, D^*\bar{D}^*$, resulting in larger cross sections.
- Wu et al. use thermal model for initial number and assume smaller cross sections for tetraquark scenario. Molecular X(3872) is produced from hadronic reactions.
- Zhang et al. use $D\bar{D}$ coalescence for molecular scenario and diquark-diquark coalescence for tetraquark scenario, based on those from AMPT.
- $\frac{X(3872)}{\psi(2S)} \approx 1$ in CMS data from Pb+Pb @ 5.02 TeV favors X(3872) to be a large hadronic molecule.

Summary

- Charged pion ratio measured by $S\pi$ RIT Collaboration $\rightarrow S_0 = 38.3 \pm 4.7$ MeV, $L = 106 \pm 37$ MeV, consistent with PREX-II but not chiral EFT + neutron stars.
- Reduced in-medium $NN \leftrightarrow N\Delta$ cross sections are needed to describe HADES pion data.
- Heavy baryonic resonances are needed for deep subthreshold Ξ production in HADES experiments.
- Enhanced Λ_c/D_0 at RHIC and LHC can be explained by heavy baryon resonances or flow effect or charm conservation \rightarrow no evidence for diquarks in QGP.
- Λ polarization freezes out early from the hadronic matter; thermal shear is important for Λ local polarization, which is automatically included in chiral kinetic approach.
- CMS data favors X(3872) to be a large hadronic molecule.

\rightarrow Studying hadron production in HIC allows to learn the nuclear equation of state, in-medium properties of hadrons and their interactions, decay modes of heavy baryonic resonances, spin transport in QGP, structures of exotic hadrons, and etc.